ISSN 1846-6168 (Print), ISSN 1848-5588 (Online)
https://doi.org/10.31803/tg-20220819001236

Original scientific paper
Received: 2022-08-19, Accepted: 2022-12-01

Improving the Performance of Patch Antenna by Applying Bandwidth Enhancement Techniques for 5G Applications

Seda Ermiş*, Murat Demirci

Abstract: In this study, various Rectangular Microstrip Antenna (RMA) designs operating at 28 GHz frequency for 5G-communication system are performed. All designs are generated and analyzed using a 3D electromagnetic simulation program, ANSYS HFSS (High-Frequency Structure Simulator). Single and array type RMA designs are constructed by using non-contact inset-fed feeding technique. Subsequently, the bandwidth of RMAs is increased by slotting on the ground surface, and adding a parasitic element to the antenna structure. Because of these analyses, for single type RMA, the bandwidth increases from 2.09 GHz to 3.45 GHz. Moreover, for 1 × 2 and 1 × 4 array type RMAs, very wide bandwidths of 7.53 GHz and 4.53 GHz, respectively, are obtained by applying bandwidth enhancement techniques. The success of the study has been demonstrated by comparing outputs of the designs with the some similar, experimental or simulation studies published in the literature.

Keywords: DGS; Rectangular Patch Antenna; 5G; 28 GHz

1 INTRODUCTION

Due to widespread use of new technology devices in recent years, the growing demand for multimedia applications and wireless data creates a significant burden on existing cellular networks. After 4G mobile network, which has been available worldwide since 2009, the 5th Generation (5G) mobile communication technology is expected to show a revolutionary development in terms of network coverage, data rate, latency, network reliability and energy efficiency [1]. With the wide-scale deployment of 5G, mobile network will be required 1000 times higher capacity and 10-100 times faster data transmission rate than the current mobile technology. This is mainly because 5G is expected to obtain a reliable communication network and stable connection not just for phones and computers, but also various types of IoT devices such as self-driving vehicles, robots, cameras or smart home gadgets [1]. Since traditional 4G/LTE network do not provide large bandwidths in giga-bits for 5G applications, several new frequency bands between 20 and 70 GHz, also known millimeter wave bands, are identified in World Radio Communication Conference 2019 (WRC-19) report [2]. However, operational frequencies around Ku band and more specifically 28/38 GHz are prominent due to their low atmospheric attenuation [3].

Antenna design for 5G devices is very crucial to perform communication in specified millimeter wave frequencies with higher gain, enhanced bandwidth and lesser radiation losses [4]. In this sense, microstrip patch antennas emerge as a strong candidate because of their numerous attractive features such as small size, low profile, ease of production, high reliability etc. In addition, microstrip antennas can tolerate path loss in terms of gain and efficiency at higher frequencies of 5G technology. However, despite of these bountiful advantages, one major problem is their narrow bandwidth [4].

To overcome this disadvantage, bandwidth enhancement techniques such as adding parasitic element, slotting shapes on the patch surface, defecting ground structure (DGS), increasing substrate thickness or coupling type of feeding are commonly used in the designs.

Literature shows that various microstrip antennas for 5G have been studied by researches recently and in some of them, bandwidth enhancement techniques have been applied. For instance, Seyyedehelnaz Ershadi et al. designed a rectangular microstrip antenna with a 4-layer substrate. The use of multiple substrates increased the bandwidth up to 21% for 28 GHz resonance frequency [5]. In 2017, Saeed Ur Rahman et al. presented a single and a 1×2 array microstrip patch antenna with the quarter wave transformation method. The 1×2 array antenna resonated at 26.5 GHz and 28.8 GHz frequencies provided 28% impedance bandwidth [6]. In the study published by Nanae Yoon and Chulhun Seo (2017), a microstrip patch antenna that communicates at 28 GHz was designed. They investigated the effects of single and double U-shaped slits on bandwidth and gain. The study showed that opening slits on the single and 2×2 array rectangular patches increased bandwidth [7]. In 2018, Kyoseung Keum and Jaehoon Choi simulated a single and a 4×4 rectangular microstrip array antenna with double U-shaped slot on the patch. The bandwidths were 3.77 GHz, and 4.71 GHz for the single and 4×4 array antennas respectively [8]. Wahaj Abbas Awan et al. designed a microstrip patch antenna operating at 28 GHz frequency for 5G technology in 2019. It was observed that the bandwidth was increased from 1.33 GHz to 1.38 GHz and the return loss was decreased from -46.97 dB to -56.95 dB by using defected ground structure (DGS) [9]. In 2020, Sharaf et al. proposed a compact dual-frequency (38/60 GHz) microstrip patch antenna for dual-band 5G mobile applications. In the design, two electromagnetically coupled patches were used and experimental results showed that achieved impedance bandwidths are about 2 GHz and 3.2 GHz in the 38 GHz and 60 GHz bands, respectively [10]. In the scientific report published by Marasco et al., in 2022, a novel, miniaturized evolved patch antenna design was introduced for flexible and bendable 5G IoT devices and its radiation properties was enhanced by using a Split Ring Resonator (SRR) in the sub-6GHz frequency band [11]. In

2022, Ezzulddin et al. fabricated and analyzed rectangular, circular and triangular microstrip patch antennas operating at 28 GHz for 5G applications. Measurements showed that achieved bandwidths of rectangular, circular and triangular microstrip patches were 0.904, 0.848 and 0.744 GHz, with the gains of 6.44, 6.03 and 5.26 dB, respectively [12].

In the published studies, some of them are summarized above, bandwidth enhancement techniques have been used, different feeding methods and substrate materials have been tested, single-element or array-shaped microstrip antenna designs have been analyzed. However, the problem is important parameters such as return loss or antenna gain decrease significantly while increasing the bandwidth.

In this study, by using ANSYS HFSS simulation program, various Rectangular Microstrip Antennas (RMA) operating at 28 GHz frequency for 5G technology are designed and analyzed. To increase antenna bandwidth, parasite patch element is added to the antenna structure and DGS technique is applied on the ground surface. When outcomes of these designs are compared with the results of the experimental and simulation studies in the literature, it has been concluded that the study is quite successful.

2 THEORETICAL BACKGROUND

Microstrip antennas are widely used due to their advantages such as lightness, small volume and low cost. In its most basic form, a RMA geometry consists of the ground plane, dielectric layer and radiating patch as shown in Fig. 1.

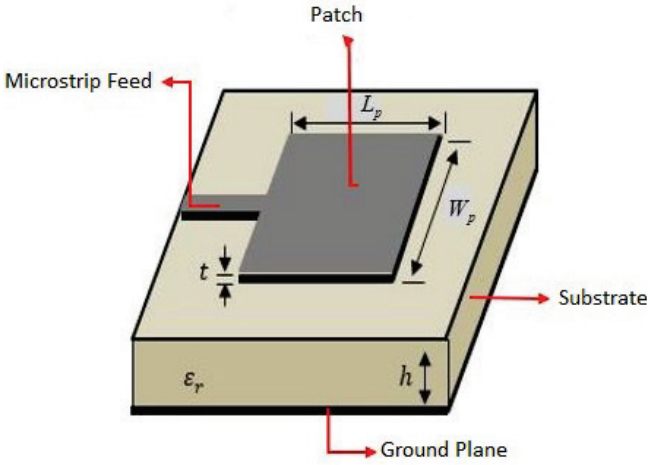

Figure 1 Rectangular Microstrip Antenna [13]

The most common patch geometry in terms of usage area is rectangular shaped patches. The width of the radiating patch, W_p, its length, L_p, the dielectric constant of the substrate (dielectric layer), ε_r and its thickness, h are shown in Fig. 1. Since thicker materials with low dielectric constant provide better radiation efficiency and wider bandwidth, a low-loss dielectric substrate Rogers RT/duroid 5880 with dielectric constant $\varepsilon_r = 2.2$ and loss tangent $\tan\delta = 0.0009$ is chosen.

As a first step, the patch width W_p and length L_p are calculated by using operation frequency f_r of the antenna and the dielectric constant of the substrate, as given in Eq. (1) [13].

$$W_p = \frac{1}{2f_r\sqrt{\mu_o\varepsilon_o}}\cdot\sqrt{\frac{2}{\varepsilon_r+1}} = \frac{\vartheta_o}{2f_r}\cdot\sqrt{\frac{2}{\varepsilon_r+1}} \tag{1}$$

Here, $\vartheta_o = c = 3\times10^8$ m/sn, $\mu_o = 4\pi\times10^{-7}$ H/m, $\varepsilon_o = 8.85\times10^{-12}$ F/m are speed of light, magnetic permeability and dielectric constant in free space respectively. The microstrip antenna has an inhomogeneous structure due to patch on the top surface, ground plane on the bottom surface and the dielectric layer between them. This structure causes the change of electrical conductivity and so, effective dielectric constant ε_{reff} is given as,

$$\varepsilon_{reff} = \frac{\varepsilon_r+1}{2} + \frac{\varepsilon_r-1}{2}\cdot\left[1+12\frac{h}{W_p}\right]^{-\frac{1}{2}} \quad \text{where } \frac{W_p}{h}>1 \tag{2}$$

Due to fringing field effect, the electrical dimension of the patch is greater than its physical dimension. The increment in length ΔL and electrical length of the patch L_{eff} are calculated by using Eqs. (3) and (4) respectively [13, 14].

$$\Delta L = \frac{0.412h\cdot(\varepsilon_{reff}+0.3)\cdot\left(\frac{W_p}{h}+0.264\right)}{(\varepsilon_{reff}-0.258)\cdot\left(\frac{W_p}{h}+0.8\right)} \tag{3}$$

$$L_{eff} = \frac{1}{2f_r\sqrt{\varepsilon_{reff}}\cdot\sqrt{\mu_o\varepsilon_o}} \tag{4}$$

Therefore, the actual length of the patch, L_p, is

$$L_p = L_{eff} - 2\Delta L = \frac{1}{2f_r\sqrt{\varepsilon_{reff}}\cdot\sqrt{\mu_o\varepsilon_o}} - 2\Delta L \tag{5}$$

Single element or array type RMAs are designed and analyzed in this study. Since non-contact inset-fed is preferred as the feeding technique, energy flow is provided indirectly by the contactless 50 Ω feeding line. The theoretical calculation of antenna and microstrip line impedances are explained in detail in Ref. 13 and 14. After the general theoretical calculations, the best gain, bandwidth and return loss values are obtained by impedance matching with the help of the software.

3 28 GHz SINGLE RMA DESIGN

RT Duroid 5880 material with dielectric constant $\varepsilon_r = 2.2$ and loss tangent $\tan\delta = 0.0009$ is used as a substrate for the 28 GHz rectangular microstrip antenna due to its low loss and low dielectric constant. The undertone substrate thickness is chosen as 0.508 mm.

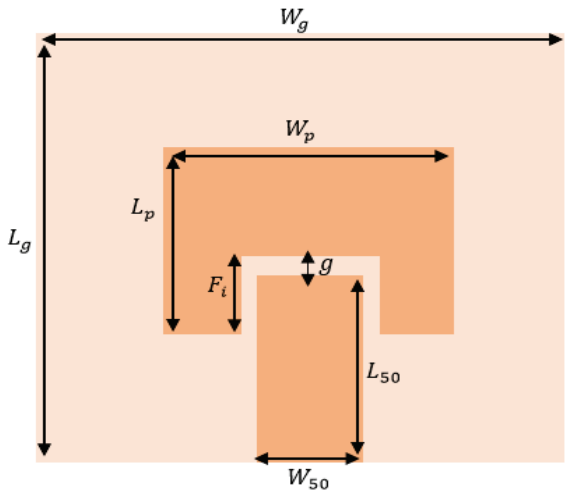

Figure 2 Top view of RMA

Table 1 Optimized dimensions of RMA (mm)

h	t	W_g	L_g	W_p	L_p	L_{50}	w_{50}	F_i	g
0.508	0.035	8	7.10	4.4	3.1	2.875	1.56	1.14	0.1

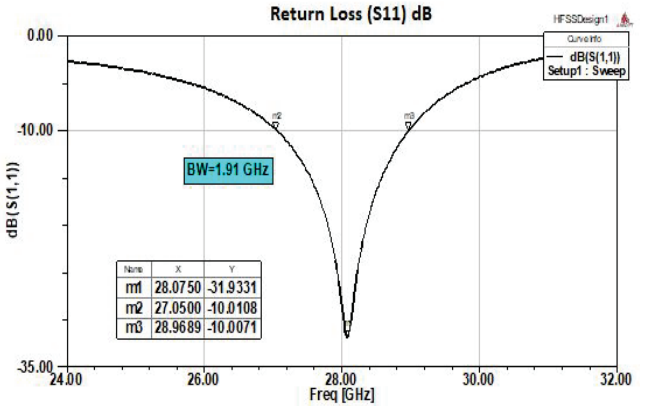

Figure 3 Return loss of RMA

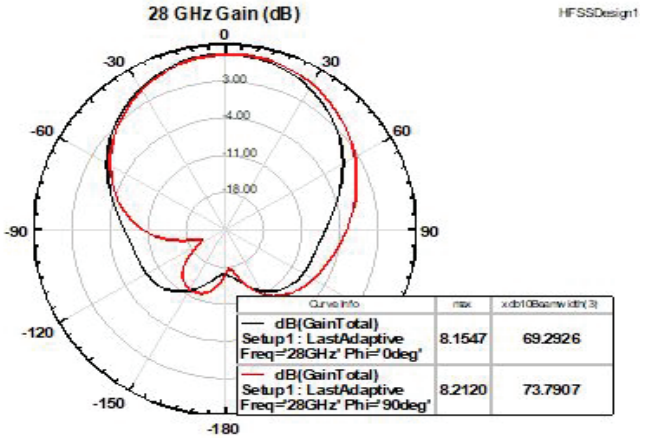

Figure 4 Polar view gain pattern of RMA

Fig. 2 shows the geometry of the RMA with non-contact inset-fed. As seen from the figure, W_p, and L_p are the patch width and length; F_i is the embedding distance of feeding line; g is gap between the feed line and the patch; h is substrate thickness; t is patch thickness; w_{50} and L_{50} are the feed line width and length; W_g and L_g are the ground surface width and length, respectively. Also, the width and length of substrate and ground surface are taken as equal. All dimensions of designed RMA are given in Tab. 1.

The return loss graph of RMA is shown in Fig. 3. RMA, emitting at a frequency of 28.075 GHz, has an impedance bandwidth of 1.91 GHz in the 27.05-28.96 GHz frequency range. As a result, designed RMA has a return loss of –31.93 dB at the frequency of 28.07 GHz, a bandwidth of 1.91 GHz and a gain of 8.20 dB (Fig. 4). As the next step, bandwidth enhancement techniques such as defecting ground structure or stacked patch technique are performed to enhance antenna bandwidth.

3.1 Application of Defected Ground Structure (DGS) and Stacked Patch Techniques for Single RMA

In microwave circuits, DGS (Defected Ground Structure) is applied by etching slots on the ground surface. Defects on the ground plane may be in the form of a single cell or periodic/aperiodic configuration of slots which depends on the application. The well-known advantages of the DGS are reducing size of component, improving bandwidth, suppressing mutual coupling or cross polarization effect and using to adjust antenna impedance for matching and for maximum power transfer.

In this part of the study, DGS is applied to the ground surface of the single RMA with non-contact inset fed by opening a slot which is in the form of a ring line aligned at the center of the patch. Bottom view of the single RMA is shown in Fig. 5(a). The radius of the ring slot is R and its width is w_R. All dimensions of the designed RMA are given in Tab. 2.

Table 2 Dimensions of RMA with Ring Shaped DGS (mm)

h	t	W_g	L_g	W_p	L_p	F_i
0.508	0.035	8	7.1	4.4	2.92	1.14
R	w_R	g	L_{50}	w_{50}		
0.6	0.3	0.1	2.875	1.56		

The more complex shape imperfections at the ground surface provide further change the path of surface currents. To see the effect of changing current distribution on the ground surface to the antenna performance parameters such as bandwidth or gain, both ring and C-shaped slots are used together as shown in Fig. 5(b). Related dimensions of the RMA for this design are given in Tab. 3.

Table 3 Dimensions of RMA with Ring / Symmetrical C Shaped DGS (mm)

h	t	W_g	L_g	W_p	L_p	F_i	R
0.508	0.035	8	7.1	4.4	2.92	1.14	0.6
w_R	L_{50}	w_{50}	g	$L_1 = L_3$	L_2	w_c	
0.3	2.875	1.56	0.1	2	1.8	0.2	

Another method to increase bandwidth of microstrip antennas is to use a stacked patch. In this method, more than one dielectric material is used and a stacked patch is added on the antenna structure. By this design, the radiation of microwave is spread and wider bandwidth can be obtained. To see the effect of stacked patch technique, two dielectric layers with same thickness ($h_1 = h_2$) and same dielectric

constant ($\varepsilon_{r1} = \varepsilon_{r2} = 2.2$) used in the structure. Main patch and contactless feed line are placed between two dielectric layers, and stacked patch is at the top of the second dielectric layer, as seen from Fig. 5(c). In addition, to combine design with the DGS, a ring shape slut is cut on the ground surface. Dimensions of the design can be found in Tab. 4 where width and length of the stacked patch are represented by W_{pp} and L_{pp} respectively.

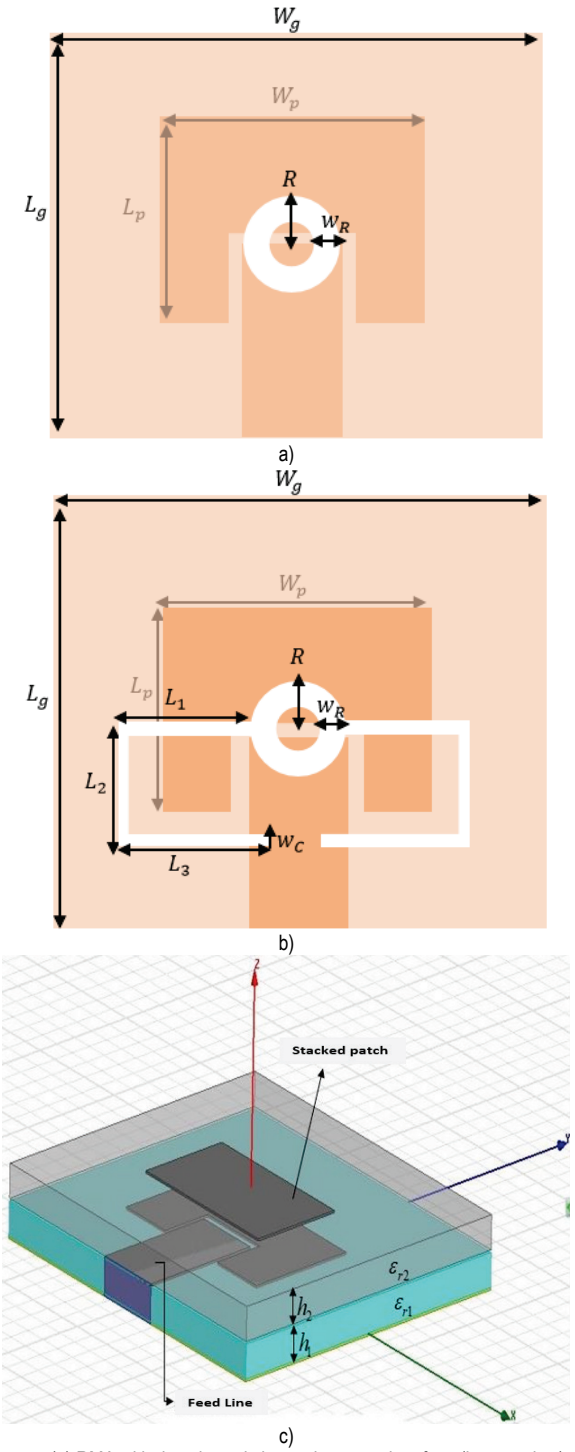

Figure 5 (a) RMA with ring shaped slot on the ground surface (bottom view); (b) RMA with ring and symmetrical C-shaped slots on the ground surface (bottom view); (c) Two-layered RMA structure combined with stacked patch and DGS.

Table 4 Dimensions of RMA with Stacked Patch and Ring Shaped DGS (mm)

h_1	h_2	t	L_{50}	w_{50}	W_p	L_p	g
0.508	0.508	0.035	2.875	1.56	4.4	2.6	0.1
L_{pp}	W_{pp}	L_g	W_g	F_i	R	w_R	
2.2	3.8	7.1	8	1.14	0.6	0.3	

Simulation results of designed RMAs given in Fig. 4, 5(a), 5(b) and 5(c) are compared and presented in Tab. 5. From the table, it is seen that the deformation on the ground surface of RMA increases bandwidth but also, it decreases antenna gain significantly. However, by the use of stacked patch technique and DGS together, clearly the widest bandwidth is obtained and significant decrease on gain is prevented.

Table 5 Comparison of Single RMA designs

Design Outputs	RMA without DGS and stacked patch	RMA with DGS		RMA with DGS and stacked patch
		RMA with ring shaped slot	RMA with ring and symmetrical C-shaped slots	
Resonance Frequency	28.075 GHz	28.03 GHz	27.99 GHz	27.96 GHz
Return Loss	–31.93 dB	–39.677dB	–28.92 dB	–26.06 dB
Gain	8.20 dB	8.08 dB	6.7 dB	8.0 dB
Bandwidth	1.91 GHz	2.09 GHz	2.69 GHz	3.45 GHz

As a next step of the study, bandwidth enhancement techniques are applied to 1 × 2 and 1 × 4 array antenna designs which are explained in the following sections.

4 28 GHz 1×2 ARRAY RMA DESIGN

The maximum gain of single microstrip patch antenna is obtained around 8 dB. As well-known from the antenna design studies, one way is creating an array structure to increase antenna directivity and gain. So, to provide higher gain, an array structure consists of two RMAs feeding by contactless microstrip lines is designed and analyzed. In Fig. 6, the geometry of the array design is shown. Dimensions of each array elements are same and width and length of the substrate and ground surface are equal.

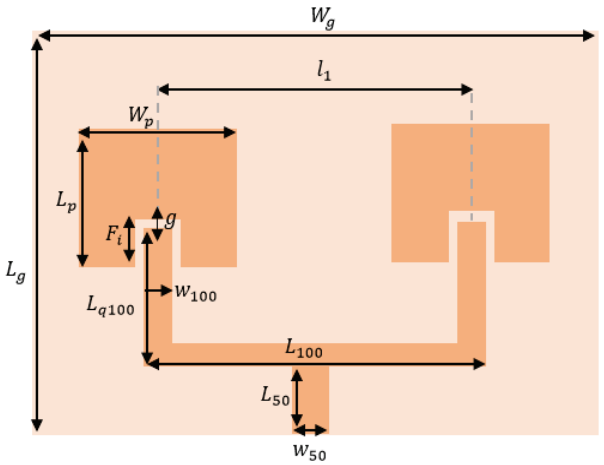

Figure 6 1×2 Array RMA dimensions

The distance (l_1) between the center points of the array elements effects the radiation pattern and changes the bandwidth and gain due to mutual coupling. Design analyses show that the widest bandwidth occurs when l_1 is chosen around 0.9λ. In addition, another issue about the design is to ensure impedance compatibility between the feed lines and patches. The impedance of the feeding line is 50 ohms and energy flow to the patches is obtained by the coupling effect of two equal 100-ohm transmission lines. The embedded distance of transmission lines into the patch has been decided by the help of simulation program to achieve impedance matching. Dimension parameters for the designed 1×2 array RMA are given in Tab. 6.

Table 6 Dimensions of 1×2 array RMA (mm)

h	t	W_g	L_g	W_p	L_p	F_i	g
0.508	0.035	18	9	4.4	2.92	0.7	0.1
L_{q100}	L_{100}	w_{100}	L_{50}	w_{50}	l_1		
1.9	9.63	1.56	2	1.56	0.9λ		

Analysis result shows that the return loss for the 28.08 GHz resonance frequency is around –44.62 dB and the bandwidth is 3.50 GHz. The gain pattern indicates that the 1×2 array RMA has 11.6 dB maximum realized gain, which is higher than the single element RMA, as expected. However, in this study, as it is aimed to increase antenna bandwidth as well as the gain, DGS and stacked patch techniques are applied to 1×2 array RMA designs which is explained in the next section.

4.1 Application of Defected Ground Structure (DGS) and Stacked Patch Techniques for 1×2 Array RMA

It has been observed that the widest bandwidth is obtained when the distance between centers of patch elements is selected as 0.9λ for the designed 1×2 Array RMA with non-contact inset-fed. In addition, ring and rod-shaped slots are cut on the ground surface and parasite patch elements are added antenna structure since it is aimed to increase the bandwidth of the 1×2 array RMA. As it can be seen from the Fig. 7(a) which is the bottom view of 1×2 array RMA, the ground surface is defected by ring and rod-shaped slots and they are located symmetrically and around the center of the two patch elements. In addition, from the Fig. 7(b), simulated 1×2 array RMA with stacked patch elements can be seen. In this design, two dielectric layers with same thickness ($h_1 = h_2$) and same dielectric constant ($\varepsilon_{r1} = \varepsilon_{r1} = 2.2$) are used.

Opening ring/rod-shaped slots on the ground surface causes a shift in the resonance frequency, and to keep resonance frequency at 28 GHz, the patch length has been reduced. While the patch length for each element is 2.92 mm in the array design without DGS, it is 2.67 mm in this design with DGS. Dimensions of the 1 × 2 array RMA represented by Fig. 7(a) and 7(b) are given in Tab. 7 where the width and length of stacked patches are represented by W_{pp} and L_{pp} respectively.

Analyses results show that by the application of stacked patches and DGS, a very wideband antenna design is made. As seen from the Fig. 8, the return loss of the design is –38.06 dB at 28 GHz and the impedance bandwidth is 7.53 GHz between 24.14 GHz and 31.66 GHz. The gain of the 1 × 2 array RMA was measured as 10.03 dB (Fig. 9). This indicates that a design that provides the desired antenna efficiency has been made, although there is a slight decrease in gain compared to previous designs.

Table 7 Dimensions of 1×2 array RMA with DGS and stacked patches (mm)

$h_2 = h_1$	t	W_g	L_g	W_p	L_p	l_1
0.508	0.035	18	9	4.4	2.7	0.9λ
L_{q100}	L_{100}	w_{100}	L_{50}	w_{50}	F_i	g
1.9	9.63	1.56	2	1.56	0.7	0.1
d	L	w_L	R	w_R	W_{pp}	L_{pp}
0.6	2.7	0.2	0.5	0.1	3.8	2

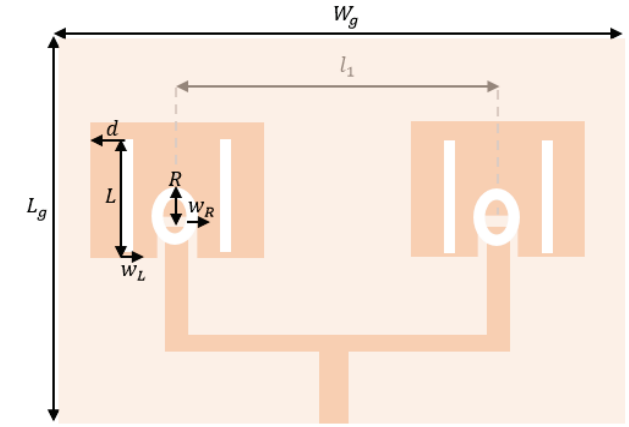

Figure 7 Bottom (a) and top (b) view of 1×2 array RMA with DGS and stacked patches

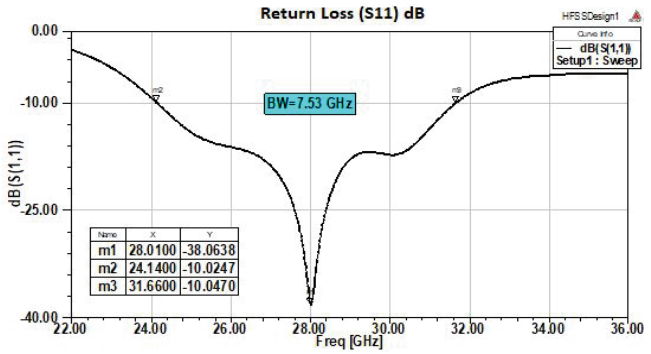

Figure 8 Return Loss of two Layer 1×2 array RMA with DGS

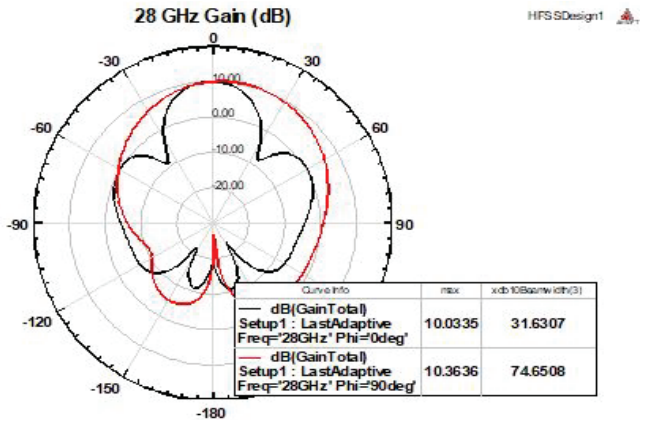

Figure 9 Gain pattern of two Layer 1 × 2 array RMA with DGS

5 28 GHz 1×4 ARRAY RMA DESIGN

In the design of 1×2 RMA array, antenna gain is varied between 10 and 11.5 dB. As a last step, 1×4 RMA array with contactless inset-fed is simulated and analyzed to increase antenna gain. Moreover, by the application of bandwidth enhancement techniques, wide band antenna is aimed at 28 GHz for 5G applications. Fig.10 shows the geometry of 1×4 array RMA design.

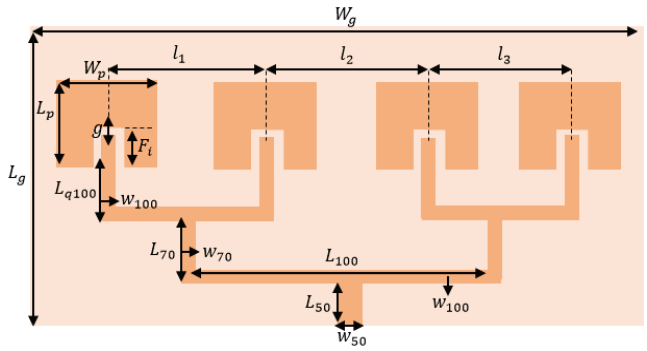

Figure 10 Geometry and dimensions of 1×4 RMA array

The distances between the centers of patch elements, given by l_1, l_2 and l_3, are defined by the help of software. The 50 ohm feed line is divided into two equivalent 100 ohm microstrip lines. Quarter wave transformation is performed by using 70 ohm microstrip line for impedance matching between two 100 ohm lines. The width and length of 70 ohm line is represented by w_{70} and L_{70}, respectively. All dimensions of the 1×4 array RMA illustrated in Fig. 10 are given in Tab. 8.

Table 8 Dimensions of 1×4 array RMA (mm)

h	t	L_g	W_g	L_p	W_p	F_i	g
0.508	0.035	11	29.7	2.9	4.35	0.8	0.1
L_{100}	L_{70}	L_{50}	L_{q100}	w_{100}	w_{70}	w_{50}	
9.63	2	2	1.9	0.45	0.9	1.56	
l_1	l_2	l_3					
0.7λ	0.5λ	0.7λ					

Analyses results show that the return loss of 1 × 4 array RMA is –43.56 dB at 27.92 GHz and –28.56 dB at 30.17 GHz. This indicates that antenna resonates at two frequencies. In addition, the bandwidth is found 4.18 GHz and maximum antenna gain is around 14 dB at 28 GHz.

5.1 Application of Defected Ground Structure (DGS) Technique for 1×4 Array RMA

In order to increase the bandwidth of the 1×4 RMA array, the ground is defected by four, concentric, double ring-shaped slots located each patch. As seen from Fig. 11, for each ring pair, the inner and outer ring radii are expressed by R_1 and R_2, with widths w_{R1} and w_{R2}, respectively. The widths and radii of slots are optimized by the HFSS software and the most suitable dimensions are defined for the best bandwidth.

The bottom view of 1×4 RMA array is given in Fig. 11 and the widths and radii of slots can be found from Tab. 9. All the other dimensions of the design are the same with the previous one, given in Tab. 8.

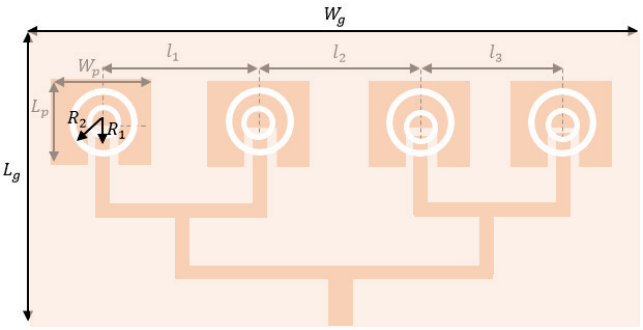

Figure 11 1×4 array RMA ground surface with DGS

Table 9 Slot dimensions of 1×4 array RMA with ring DGS (mm)

Inner Ring Radius	R_1	0.5
Inner Ring Width	w_{R1}	0.1
Outer Ring Radius	R_2	0.8
Outer Ring Width	w_{R2}	0.1

Like the previous one, in this design antenna resonates at two frequencies, which are 28.12 GHz, and 30.63 GHz. Return loss and antenna gain are –31.53 dB and 13.34 dB. As expected, gain slightly decreases due to defected ground surface. However, the bandwidth of RMA increases to 4.53 GHz.

6 RESULTS AND DISCUSSION

To see the effect of the bandwidth enhancement techniques, a comparison of all design cases with respect to antenna output parameters is given in Tab. 10 and important conclusions of the study are summarized as follows:

1) For all design cases, defected ground surface and parasitic patch element provide wider bandwidth at the operating frequency as seen from Tab. 10.
2) According to Tab. 5, if only DGS is applied to single RMA, antenna gain is reduced significantly due to complex shape imperfection and radiation loss. To avoid this situation, the combination of DGS and stacked patch technique with multiple layer dielectric substrates is performed in the design and it is observed that wider bandwidth can be achieved with slight decrease on gain. Therefore, it can be said that overall performance of

single RMA is improved by using these bandwidth enhancement techniques.

3) To provide higher gain, one well-known method is to increase antenna directivity by arraying. To do that, 1×2 and 1×4 RMA arrays are designed and analyzed. Both two array designs improve antenna gain with respect to the single RMA, as expected.
4) By applying DGS and adding parasitic patch element with multiple layer substrates to 1×2 RMA array structure, the best bandwidth (≈7.5 GHz), which is more than twice of the bandwidth of the design without using DGS and parasitic patch elements (≈3.5 GHz), is obtained. The gain for this design is around 10.3 dB which is slightly less (≈1.3dB) than 1 × 2 RMA array design without using any bandwidth enhancement methods.
5) The highest gain (≈14dB) is obtained by the 1 × 4 RMA array configuration, as expected. By applying DGS to the design, slight increase on bandwidth (9.7%) and decrease on gain (0.2 dB) is observed. Stacked patch technique is not implemented to the design to avoid high degree of design complexity, high loss and very dispersed radiation pattern which causes multiple resonance frequency.
6) For all designs, regardless of single or array RMA configurations, by the application of DGS and stacked patch, loss is increased because of adding some components such as multiple dielectric substrate or parasitic patch element to the design and deformation on the ground plane. However, for all designs, loss level is less than –10 dB so it is in acceptable range for application.

As a last step of this study, obtained results of the analyses of single and 1×2/1×4 array RMAs are compared with some similar publications in the literature and expressed in Tab. 11 and 12. As seen from Tab. 11, using the combination of DGS and stacked patch technique obviously increases bandwidth and it prevents significant decrease on gain.

Table 10 Comparison of outputs of Single and Array RMA designs in this work

Design Outputs	Single RMA without DGS and stacked patch	Single RMA with DGS and stacked patch	1 × 2 Array RMA without DGS and stacked patch	1 × 2 Array RMA with DGS and stacked patch	1 × 4 Array RMA without DGS	1 × 4 Array RMA with DGS
Resonance Frequency	28.075 GHz	27.96 GHz	28.08 GHz	28.01 GHz	27.92 GHz	28.12GHz
Return Loss	–31.93 dB	–26.06 dB	–44.62 dB	–38.06 dB	–43.57 dB	–31.53 dB
Gain	8.20 dB	8.0 dB	11.62 dB	10.36 dB	14.02 dB	13.80 dB
Bandwidth	1.91 GHz	3.45 GHz	3.50 GHz	7.53 GHz	4.13 GHz	4.53 GHz

Table 11 Comparison of Single RMA simulation results with similar studies in the literature

Reference Study	Resonance Frequency	Return Loss	Bandwidth	Gain
[12]	28.04 GHz (Rectangular Patch)	–14.81 dB	0.904 GHz	6.44 dB
	28.06 GHz (Circular Patch)	–24.12 dB	0.848 GHz	6.03 dB
	28.10 GHz (Triangular Patch)	–18.80 dB	0.744 GHz	5.26 dB
[15]	28 GHz	–39.36 dB	2.48 GHz	6.37 dB
[16]	28.3 GHz	≈–38 dB	2.4 GHz	5.56 dB
[17]	28 GHz	–40 dB	1.3GHz	7.6 dB
[18]	28 GHz	≈–28 dB	2.66 GHz	5.82 dB
[19]	28 GHz	–24 dB	2.24 GHz	7.86 dB
[20]	27.9 GHz	–15.35 dB	≈0.5 GHz	6.92 dB
[21]	28.96 GHz	–19.12 dB	3.93 GHz	6.05 dB
[22]	28 GHz	–59.17 dB	1.3 GHz	10.1 dB
Single RMA with DGS and Stacked Patch in this study	27.96 GHz	–26.06 dB	3.45 GHz	8.0 dB

Table 12 Comparison of Array RMA simulation results with similar studies in the literature

Reference Study	Array Type	Resonance Frequency	Return Loss	Bandwidth	Gain
[17]	1 × 4	28 GHz	–25.8 dB	1.2 GHz	13.5 dB
[20]	1 × 2	27.94 GHz	–13.77 dB	≈0.5 GHz	9.52 dB
	1 × 4	27.53 GHz	–21.44 dB	≈1 GHz	11.2 dB
[21]	1 × 2	29.06 GHz	–19.31 dB	2.36 GHz	7.15 dB
	1 × 4	28.85 GHz	–24.56 dB	1.17 GHz	10.27 dB
[22]	2 × 2	28 GHz	–61.19 dB	1.3 GHz	15.31 dB
[23]	1 × 2 (MIMO)	28 GHz	≈–17 dB	2.GHz	9.4 dB
Array RMA with DGS and Stacked Patch in this study	1 × 2	28.01 GHz	–38.06 dB	7.53 GHz	10.36 dB
Array RMA with DGS in this study	1 × 4	28.12 GHz	–31.53 dB	4.53 GHz	13.8 dB

Of course, it is possible to obtain wider bandwidth with lower gain or vice versa by applying different design techniques, which depends on the application and major consideration of the design. However, the overall aim of this work is to improve antenna performance by using bandwidth enhancement techniques in the design and results show that in the desired frequency range, efficient designs with wide bandwidth and good gain for single or array type RMAs are achieved for the applications of 5G.

7 REFERENCES

[1] Agiwal, M., Roy, A., & Saxena, N. (2016). Next Generation 5G Wireless Networks: A Comprehensive Survey. *IEEE Commun. Surv. Tutorials, 18*(3), 1617-1655.

https://doi.org/10.1109/COMST.2016.2532458
[2] Marcus, M. J. (2019). ITU WRC-19 Spectrum Policy Results. *IEEE Wireless Communications*, 26(6). 4-5. https://doi.org/10.1109/MWC.2019.8938175
[3] Banday, Y., Rather, G. Md., & Begh, G. R. (2019). Effect of Atmospheric Absorption on Millimeter Wave Frequencies for 5G Cellular Networks. *IET Communications, 13*(3), 265-270. https://doi.org/10.1049/iet-com.2018.5044
[4] Wang, X. et al. (2018). Millimeter Wave Communication: A Comprehensive Survey. *IEEE Communications Surveys & Tutorials, 20*(3), 1616-1653. https://doi.org/10.1109/COMST.2018.284432
[5] Ershadi, S., Keshtkar, A., Ershadi, S., Abdelrahman, A. H., Yu, X., & Xin, H. (2016). Wideband subarray design for 5G an antenna arrays. *2016 URSI Asia-Pacific Radio Science Conference (URSI AP-RASC)*, 185-187. https://doi.org/10.1109/URSIAP-RASC.2016.7601266
[6] Rahman, S. U., Cao, Q., Hussain, I., Khalil, H., Zeeshan, M., & Nazar, W. (2017). Design of rectangular patch antenna array for 5G wireless communication. *Progress in Electromagnetics Research Symposium - Spring (PIERS2017)*, 1558-1562. https://doi.org/10.1109/PIERS.2017.8261995
[7] Yoon, N. & Seo, C. (2017). A 28-GHz Wideband 2×2 U-slot patch array antenna. *J. Electromagn. Eng. Sci.*, 17(1), 133-137. https://doi.org/10.5515/JKIEES.2017.17.3.133
[8] Keum, K. & Choi, J. (2018). A 28 GHz 4 × 4 U-Slot Patch Array Antenna for mm-wave Communication. *International Symposium on Antennas and Propagation (ISAP2018)*, 1-2.
[9] Awan, W. A., Zaidi, A., & Baghdad, A. (2019). Patch Antenna with Improved Performance Using DGS for 28 GHz Applications. *International Conference on Wireless Technologies, Embedded and Intelligent Systems (WITS2019)*, 1-4. https://doi.org/10.1109/WITS.2019.8723828
[10] Sharaf, M. H., Zaki, A. I., Hamad, R. K., & Omar, M. M. M. (2020). A Novel Dual-Band (38/60 GHz) Patch Antenna for 5G Mobile Handsets. *Sensors, 20*(9), 2541. https://doi.org/10.3390/s20092541
[11] Marasco, I., Niro, G., Mastronardi, V. M. et al. (2022). A Compact Evolved Antenna for 5G Communications. *Sci Rep 12*, 10327. https://doi.org/10.1038/s41598-022-14447-9
[12] Ezzulddin, S. K., Hasan, S. O., & Ameen, M. M. (2022). Microstrip Patch Antenna Design, Simulation and Fabrication for 5G Applications. *Simulation Modelling Practice and Theory, 116*, 102497. https://doi.org/10.1016/j.simpat.2022.102497
[13] Balanis, C. (1982). *Antenna Theory: analysis and design*. Balanis, C. A. SERBIULA (sistema Libr. 2.0).
[14] Pozar, D. M. (2012). *Microwave Engineering*. Fourth edition. Hoboken, NJ, Wiley.
[15] Kaeib, A. F., Shebani, N. M., & Zarek, A. R. (2019). Design and Analysis of a Slotted Microstrip Antenna for 5G Communication Networks at 28 GHz. *The 19th International Conference on Sciences and Techniques of Automatic Control and Computer Engineering (STA)*, 648-653. https://doi.org/10.1109/STA.2019.8717292
[16] Adedotun, O. K. & Johnbosco, A. I. E. (2017). Design and Optimization of a Square Patch Atenna for Milimeter Wave Applications. *International Journal of Science and Research (IJSR), 6*(4), 2192-2194.
[17] Khattak, M. I., Sohail, A., Khan, U., Barki, Z., & Witjaksono, G. (2019). Elliptical Slot Circular Patch Antenna Array with Dual Band Behavior for Future 5G Mobile Communication Networks. *Progress in Electromagnetics Research C, 89*, 133-147. https://doi.org/10.2528/PIERC18101401
[18] Rahman, A., Ng, M., Yi, A., Ahmed, U., Alam, T., Singh, M. J., & Islam, M. T. (2016). A Compact 5G Antenna Printed on Manganese Zinc Ferrite Substrate Material. *IEICE Electronics Express, J-STAGE, 13*(11), 20160377. https://doi.org/10.1587/elex.13.20160377
[19] Rahman, S. U., Cao, Q., Hussain, I., Khalil, H., Zeeshan, M., & Nazar, W. (2017). Design of Rectangular Patch Antenna Array for 5G Wireless Communication. *Progress in Electromagnetics Research Symposium - Spring (PIERS2017)*, 1558-1562. https://doi.org/10.1109/PIERS.2017.8261995
[20] EL Mashade, M. B. & Hegazy, E. A. (2018). Design and Analysis of 28 GHz Rectangular Microstrip Patch Array Antenna. *WSEAS Transactions on Communications, 17*(1), 9.
[21] Prabu, R. T. & Bai, V. T. (2019). Design of Eight Element Phased Array Microstrip Patch Antenna for 5G Application. *International Journal of Recent Technology and Engineering (IJRTE), 8*(1), 936-941.
[22] Soliman, Md. M., Imran, A. Z. Md., & Ullah, K. S. (2019). Highly Efficient 2×2 Antenna Array at 28 GHz and 38 GHz for 5G Applications. *In 2019 International Conference on Innovation in Engineering and Technology (ICIET)*, 23-24 December. https://doi.org/10.1109/ICIET48527.2019.9290692
[23] Ardianto, F. W., Lanang, F. F., Renaldy, S., & Yunita, T. (2018). Design Mimo Antenna with U-Slot Rectangular Patch Array for 5G Applications. In *2018 International Symposium on Antennas and Propagation (ISAP)* IEEE, 1-2.

Authors' contacts:

Seda Ermiş, Asst. Prof. Dr.
(Corresponding author)
Osmaniye Korkut Ata University, Engineering Faculty,
Electrical and Electronics Engineering Department,
80000, Merkez, Osmaniye, Turkey
sedaermis@osmaniye.edu.tr

Murat Demirci
Osmaniye Korkut Ata University, Engineering Faculty,
Electrical and Electronics Engineering Department,
80000, Merkez, Osmaniye, Turkey